formation concerning the function of COX-1, such as for the mucosal protection of the stomach and blood flow maintenance, has been available (38). Recently, COX-1, but not COX-2, was reported to show involvement in brain inflammation (39, 40), and, importantly, COX-1 expression is regulated in PC12 cells in response to NGF stimulation (41, 42), suggesting that COX-1 is associated with neuronal differentiation. In our study, down-regulation of COX-1 using COX-1 siRNA rescued the abnormal phenotypes observed in NF1-K_D cells; thus, COX-1 may be a candidate clinical target for NF1-related disease pathogenesis. The precise mechanism of COX-1 expression and function in neuronal differentiation related to NF1 pathogenesis remains to be clarified in future investigations.

In this study, we found that COX-1 expression was regulated by GR, and dynein IC2-GR-COX-1 signaling was up-regulated in NF1-K_D cells. In NF1-K_D cells, suppression of dynein IC2 inhibits nuclear translocation of GR and decreases COX-1 expression. However, which dynein isoform is associated with GR transport and what mechanisms of dynein phosphorylation are involved remain unclear. Because no change in COX-1 expression was induced by dynein IC2-C siRNA treatment, dynein IC2-B rather than dynein IC2-C may be associated with GR translocation. Interestingly, COX-1 siRNA effectively recovered the neurite retraction of NF1-K_D cells. We speculate that prostaglandins up-regulated by COX-1 may be associated with neurite outgrowth. Four prostaglandin E2 (PGE2) receptors, EP1, EP2, EP3, and EP4, have been identified (43), and EP2 and EP3 expression was up-regulated at 48 h and 72 h, respectively, in our DNA array analysis. EP3 has been reported to couple with G protein receptors to activate RhoA (44, 45), which was also identified as up-regulated in NF1-K_D HeLa cells in our previous report (10). Several studies show that activation of RhoA mediates neurite retraction in PC12 cells (44, 45). Therefore, up-regulation of COX-1 in NF1-K_D cells is speculated to promote PGE2 synthesis and the activation of RhoA via EP3, followed by the inhibition of neurite outgrowth in PC12 cells. COX-1 knockdown may also block this signaling activation and improve the abnormal phenotype observed in NF1-K_D cells.

In NF1 patients, a cognitive deficit has frequently been found as one of the typical NF1-related phenotypes and suggested that neurofibromin plays an essential role in neuronal cells. NF1 heterozygous (Nf1±) mice indicated spatial learning disability by the Morris water maze test (3, 46) and other reports also showed retraction of neurite and growth corn in NF1 heterozygous (Nf1±) hippocampal neurons (47). Therefore abnormal neuronal assembly such as neurite retraction is related to learning disability in NF1 patients. In our study, we used PC12 cells as model cells of neuronal differentiation to evaluate the function of neurofibromin. We firstly demonstrated that neurite retraction observed in NF1-K_D cells is recovered by cotransfected dynein IC2-C siRNA (Figs 5*B*, 5*C*) or COX-1 siRNA (Figs. 6*G*, 6*H*). These experimental evidences may explain the possible functional relevance of the abnormal regulation of dynein IC2-GR-COX1 signaling to the NF1 pathology. Further studies based on our findings will elucidate the mechanism of NF1-related neuronal pathogenesis, such as learning disability.

This study is the first demonstration using an integrated proteomics approach that the specific signaling of dynein IC2-GR-COX-1 extracted from NF1-disease model neuronal cells may be an important mechanism of NF1-related pathogenesis. Drugs inhibiting this signaling such as specific COX-1 inhibitors may be useful candidates for the treatment of NF1 patients with neuronal abnormalities.

Acknowledgments—We thank the entire staff of the Department of Tumor Genetics and Biology at Kumamoto University for helpful support, especially M. Nagai for experimental assistances, and C. Midorikawa, K. Tanoue, and M. Nakamura for secretarial support.

* This study was supported by grants from the Ministry of Health, Labor and Welfare of Japan (NA), Kiban B Research (NA), Houga Research (NA), Exploratory Research for Young Scientists (B) (DK) from the Ministry of Education, Science, Sports, and Culture of Japan; and from the COE project B of Kumamoto University for proteomic research and education (NA).

ZSI

AQ: C

S This article contains supplemental Figs. S1 to S4 and Tables S1 to S7.

‖ To whom correspondence should be addressed: Department of Tumor Genetics and Biology, Graduate school of Medical Sciences, Kumamoto University, 1-1-1, Honjo, Kumamoto 860-8556, Japan. Tel.: +81-96-373-5119; Fax: +81-96-373-5210; E-mail: nori@gpo.kumamoto-u.ac.jp.

** These authors contributed equally to this work.

Authors' present addresses: S Mizuguchi, Dept. Neurosurgery, Faculty of Medicine, University of Miyazaki, 5200 Kihara Kiyotake Miyazaki, 889-1692, Japan; T Morikawa, Mitsubishi Chemical Medience Corporation, 14, Sunayama, Kamisu, Ibaraki 314-0255, Japan.; U. Midorikawa, Healthcare Systems Laboratories, Sharp Corp. 1-9-2, Nakase, Mihama-ku, Chiba, 261-8520, Japan; A.C. Yoshizawa, Koichi Tanaka Laboratory of Advanced Science and Technology, Shimadzu Corporation, Nishinokyo-Kuwabara-cho, Nakagyo-ku, Kyoto 604-8511, Japan.

REFERENCES

1. Stephens, K., Riccardi, V. M., Rising, M., Ng, S., Green, P., Collins, F. S., Rediker, K. S., Powers, J. A., Parker, C., and Donis-Keller, H. (1987) Linkage studies with chromosome 17 DNA markers in 45 neurofibromatosis 1 families. *Genomics* **1,** 353–357
2. Cawthon, R. M., Weiss, R., Xu, G. F., Viskochil, D., Culver, M., Stevens, J., Robertson, M., Dunn, D., Gesteland, R., O'Connell, P., *et al.* (1990) A major segment of the neurofibromatosis type 1 gene: cDNA sequence, genomic structure, and point mutations. *Cell* **62,** 193–201
3. Costa, R. M., Federov, N. B., Kogan, J. H., Murphy, G. G., Stern, J., Ohno, M., Kucherlapati, R., Jacks, T., and Silva, A. J. (2002) Mechanism for the learning deficits in a mouse model of neurofibromatosis type 1. *Nature* **415,** 526–530
4. Guo, H. F., Tong, J., Hannan, F., Luo, L., and Zhong, Y. (2000) A neurofibromatosis-1-regulated pathway is required for learning in Drosophila. *Nature* **403,** 895–898
5. Gregory, P. E., Gutmann, D. H., Mitchell, A., Park, S., Boguski, M., Jacks, T., Wood, D. L., Jove, R., and Collins, F. S. (1993) Neurofibromatosis type 1 gene product (neurofibromin) associates with microtubules. *Somat. Cell Mol. Genet.* **19,** 265–274
6. Yunoue, S., Tokuo, H., Fukunaga, K., Feng, L., Ozawa, T., Nishi, T., Kikuchi, A., Hattori, S., Kuratsu, J., Saya, H., and Araki, N. (2003) Neurofibroma-

tosis type I tumor suppressor neurofibromin regulates neuronal differentiation via its GTPase-activating protein function toward Ras. *J. Biol. Chem.* **278,** 26958–26969
7. Patrakitkomjorn, S., Kobayashi, D., Morikawa, T., Wilson, M. M., Tsubota, N., Irie, A., Ozawa, T., Aoki, M., Arimura, N., Kaibuchi, K., Saya, H., and Araki, N. (2008) Neurofibromatosis type 1 (NF1) tumor suppressor, neurofibromin, regulates the neuronal differentiation of PC12 cells via its associating protein, CRMP-2. *J. Biol. Chem.* **283,** 9399–9413
8. Kobayashi, D., Kumagai, J., Morikawa, T., Wilson-Morifuji, M., Wilson, A., Irie, A., and Araki, N. (2009) An integrated approach of differential mass spectrometry and gene ontology analysis identified novel proteins regulating neuronal differentiation and survival. *Mol. Cell. Proteomics* **8,** 2350–2367
9. Shilov, I. V., Seymour, S. L., Patel, A. A., Loboda, A., Tang, W. H., Keating, S. P., Hunter, C. L., Nuwaysir, L. M., and Schaeffer, D. A. (2007) The Paragon Algorithm, a next generation search engine that uses sequence temperature values and feature probabilities to identify peptides from tandem mass spectra. *Mol. Cell. Proteomics* **6,** 1638–1655
10. Ozawa, T., Araki, N., Yunoue, S., Tokuo, H., Feng, L., Patrakitkomjorn, S., Hara, T., Ichikawa, Y., Matsumoto, K., Fujii, K., and Saya, H. (2005) The neurofibromatosis type 1 gene product neurofibromin enhances cell motility by regulating actin filament dynamics via the Rho-ROCK-LIMK2-cofilin pathway. *J. Biol. Chem.* **280,** 39524–39533
11. Ha, J., Lo, K. W., Myers, K. R., Carr, T. M., Humsi, M. K., Rasoul, B. A., Segal, R. A., and Pfister, K. K. (2008) A neuron-specific cytoplasmic dynein isoform preferentially transports TrkB signaling endosomes. *J. Cell Biol.* **181,** 1027–1039
12. Pfister, K. K., Salata, M. W., Dillman, J. F., 3rd, Vaughan, K. T., Vallee, R. B., Torre, E., and Lye, R. J. (1996) Differential expression and phosphorylation of the 74-kDa intermediate chains of cytoplasmic dynein in cultured neurons and glia. *J. Biol. Chem.* **271,** 1687–1694
13. Picard, D., and Yamamoto, K. R. (1987) Two signals mediate hormone-dependent nuclear localization of the glucocorticoid receptor. *EMBO J.* **6,** 3333–3340
14. Madan, A. P., and DeFranco, D. B. (1993) Bidirectional transport of glucocorticoid receptors across the nuclear envelope. *Proc. Natl. Acad. Sci. U.S.A.* **90,** 3588–3592
15. Galigniana, M. D., Radanyi, C., Renoir, J. M., Housley, P. R., and Pratt, W. B. (2001) Evidence that the peptidylprolyl isomerase domain of the hsp90-binding immunophilin FKBP52 is involved in both dynein interaction and glucocorticoid receptor movement to the nucleus. *J. Biol. Chem.* **276,** 14884–14889
16. Harrell, J. M., Murphy, P. J., Morishima, Y., Chen, H., Mansfield, J. F., Galigniana, M. D., and Pratt, W. B. (2004) Evidence for glucocorticoid receptor transport on microtubules by dynein. *J. Biol. Chem.* **279,** 54647–54654
17. Wochnik, G. M., Ruegg, J., Abel, G. A., Schmidt, U., Holsboer, F., and Rein, T. (2005) FK506-binding proteins 51 and 52 differentially regulate dynein interaction and nuclear translocation of the glucocorticoid receptor in mammalian cells. *J. Biol. Chem.* **280,** 4609–4616
18. Vaughan, P. S., Leszyk, J. D., and Vaughan, K. T. (2001) Cytoplasmic dynein intermediate chain phosphorylation regulates binding to dynactin. *J. Biol. Chem.* **276,** 26171–26179
19. Schnapp, B. J., and Reese, T. S. (1989) Dynein is the motor for retrograde axonal transport of organelles. *Proc. Natl. Acad. Sci. U.S.A.* **86,** 1548–1552
20. Schroer, T. A., Steuer, E. R., and Sheetz, M. P. (1989) Cytoplasmic dynein is a minus end-directed motor for membranous organelles. *Cell* **56,** 937–946
21. Hirokawa, N., Niwa, S., and Tanaka, Y. (2010) Molecular motors in neurons: transport mechanisms and roles in brain function, development, and disease. *Neuron* **68,** 610–638
22. Pfister, K. K., Shah, P. R., Hummerich, H., Russ, A., Cotton, J., Annuar, A. A., King, S. M., and Fisher, E. M. (2006) Genetic analysis of the cytoplasmic dynein subunit families. *PLoS Genet* **2,** e1
23. Salata, M. W., Dillman, J. F., 3rd, Lye, R. J., and Pfister, K. K. (2001) Growth factor regulation of cytoplasmic dynein intermediate chain subunit expression preceding neurite extension. *J. Neurosci. Res.* **65,** 408–416
24. Bader, J. R., Kasuboski, J. M., Winding, M., Vaughan, P. S., Hinchcliffe, E. H., and Vaughan, K. T. (2011) Polo-like kinase1 is required for recruitment of dynein to kinetochores during mitosis. *J. Biol. Chem.* **286,** 20769–20777
25. Karki, S., Tokito, M. K., and Holzbaur, E. L. (1997) Casein kinase II binds to and phosphorylates cytoplasmic dynein. *J. Biol. Chem.* **272,** 5887–5891
26. Ikeda, K., Zhapparova, O., Brodsky, I., Semenova, I., Timauer, J. S., Zaliapin, I., and Rodionov, V. (2011) CK1 activates minus-end-directed transport of membrane organelles along microtubules. *Mol. Biol. Cell* **22,** 1321–1329
27. Anacker, C., Zunszain, P. A., Cattaneo, A., Carvalho, L. A., Garabedian, M. J., Thuret, S., Price, J., and Pariante, C. M. (2011) Antidepressants increase human hippocampal neurogenesis by activating the glucocorticoid receptor. *Mol. Psychiatry* **16,** 738–750
28. Kim, Y. S., Jang, S. W., Sung, H. J., Lee, H. J., Kim, I. S., Na, D. S., and Ko, J. (2005) Role of 14-3-3 eta as a positive regulator of the glucocorticoid receptor transcriptional activation. *Endocrinology* **146,** 3133–3140
29. Marnett, L. J., Rowlinson, S. W., Goodwin, D. C., Kalgutkar, A. S., and Lanzo, C. A. (1999) Arachidonic acid oxygenation by COX-1 and COX-2. Mechanisms of catalysis and inhibition. *J. Biol. Chem.* **274,** 22903–22906
30. Smith, W. L., Garavito, R. M., and DeWitt, D. L. (1996) Prostaglandin endoperoxide H synthases (cyclooxygenases)-1 and -2. *J. Biol. Chem.* **271,** 33157–33160
31. Sun, H., Sheveleva, E., and Chen, Q. M. (2008) Corticosteroids induce cyclooxygenase 1 expression in cardiomyocytes: role of glucocorticoid receptor and Sp3 transcription factor. *Mol. Endocrinol.* **22,** 2076–2084
32. Smith, W. L., DeWitt, D. L., and Garavito, R. M. (2000) Cyclooxygenases: structural, cellular, and molecular biology. *Annu. Rev. Biochem.* **69,** 145–182
33. Dang, I., and De Vries, G. H. (2011) Aberrant cAMP metabolism in NF1 malignant peripheral nerve sheath tumor cells. *Neurochem. Res.* **36,** 1697–1705
34. Park, S. W., Kim, H. S., Choi, M. S., Jeong, W. J., Heo, D. S., Kim, K. H., and Sung, M. W. (2011) The effects of the stromal cell-derived cyclooxygenase-2 metabolite prostaglandin E2 on the proliferation of colon cancer cells. *J. Pharmacol. Exp. Ther.* **336,** 516–523
35. Rundhaug, J. E., Pavone, A., Kim, E., and Fischer, S. M. (2007) The effect of cyclooxygenase-2 overexpression on skin carcinogenesis is context dependent. *Mol. Carcinog.* **46,** 981–992
36. Masferrer, J. L., Zweifel, B. S., Manning, P. T., Hauser, S. D., Leahy, K. M., Smith, W. G., Isakson, P. C., and Seibert, K. (1994) Selective inhibition of inducible cyclooxygenase 2 in vivo is antiinflammatory and nonulcerogenic. *Proc. Natl. Acad. Sci. U.S.A.* **91,** 3228–3232
37. Muraki, C., Ohga, N., Hida, Y., Nishihara, H., Kato, Y., Tsuchiya, K., Matsuda, K., Totsuka, Y., Shindoh, M., and Hida, K. (2012) Cyclooxygenase-2 inhibition causes antiangiogenic effects on tumor endothelial and vascular progenitor cells. *Int. J. Cancer* **130,** 59–70
38. Peskar, B. M. (2001) Role of cyclooxygenase isoforms in gastric mucosal defence. *J. Physiol. Paris* **95,** 3–9
39. Anrather, J., Gallo, E. F., Kawano, T., Orio, M., Abe, T., Gooden, C., Zhou, P., and Iadecola, C. (2011) Purinergic signaling induces cyclooxygenase-1-dependent prostanoid synthesis in microglia: roles in the outcome of excitotoxic brain injury. *PLoS One* **6,** e25916
40. Choi, S. H., Aid, S., and Bosetti, F. (2009) The distinct roles of cyclooxygenase-1 and -2 in neuroinflammation: implications for translational research. *Trends Pharmacol. Sci.* **30,** 174–181
41. Kaplan, M. D., Olschowka, J. A., and O'Banion, M. K. (1997) Cyclooxygenase-1 behaves as a delayed response gene in PC12 cells differentiated by nerve growth factor. *J. Biol. Chem.* **272,** 18534–18537
42. Yung, H. S., Chow, K. B., Lai, K. H., and Wise, H. (2009) Gi-coupled prostanoid receptors are the likely targets for COX-1-generated prostanoids in rat pheochromocytoma (PC12) cells. *Prostaglandins Leukot. Essent. Fatty Acids* **81,** 65–71
43. Sugimoto, Y., and Narumiya, S. (2007) Prostaglandin E receptors. *J. Biol. Chem.* **282,** 11613–11617
44. Tamiji, J., and Crawford, D. A. (2010) Prostaglandin E(2) and misoprostol induce neurite retraction in Neuro-2a cells. *Biochem. Biophys. Res. Commun.* **398,** 450–456
45. Katoh, H., Negishi, M., and Ichikawa, A. (1996) Prostaglandin E receptor EP3 subtype induces neurite retraction via small GTPase Rho. *J. Biol. Chem.* **271,** 29780–29784
46. Silva, A. J., Frankland, P. W., Marowitz, Z., Friedman, E., Laszlo, G. S., Cioffi, D., Jacks, T., and Bourtchuladze, R. (1997) A mouse model for the learning and memory deficits associated with neurofibromatosis type I. Nat. *Genet.* **15,** 281–284
47. Brown, J. A., Gianino, S. M., and Gutmann, D. H. (2010) Defective cAMP generation underlies the sensitivity of CNS neurons to neurofibromatosis-1 heterozygosity. *J. Neurosci.* **30,** 5579–5589

Integrated proteomics identified novel activation of dynein IC2-GR-COX-1 signaling in NF1 disease model cells

Mio Hirayama1*, Daiki Kobayashi1*, Souhei Mizuguchi1, Takashi Morikawa1, Megumi Nagayama1, Uichi Midorikawa1, Masayo M. Wilson1, Akiko N. Nambu1, Akiyasu C. Yoshizawa2, Shin Kawano3, and Norie Araki1**

Supplemental Informations

Supplemental Tables: S1-S7

Supplemental Figures: S1-S4

Supplemental Tables

Table S1

List of the identified molecules and associated data obtained by 2D-DIGE, iTRAQ, and DNA array.

Every annotation with merged data was obtained using iPEACH software.

UniProt release 2012_02 was used for the annotation.

*iPEACH indices (z) were calculated as follows:

$z = \Sigma\{ |log_2(x_0)| + |log_2 (x_{24})| + |log_2 (x_{48})| + |log_2 (x_{72})|\}$

x = ratio of gene or protein expression in the NF1 siRNA treatment to control siRNA treatment groups

Each suffix indicates stimulation time.

Column legends were shown in the table below:

Column legends	
Entrez_ID	Entrez_ID
UniProt_ID	UniProt_ID
Review	The data source from SwissProt or trEMBL
UniProt_Accession	UniProt_Accession
Gene_Name	Gene_Name from UniProt
Name	Name
Method/Master_Spot_Number	Method/Master_Spot_Number
Ratio_si/c_0h	Ratio obtained from DNA microarray, 2D-DIGE, iTRAQ (ESI / MALDI) data at each time point
Ratio_si/c_24h	
Ratio_si/c_48h	
Ratio_si/c_72h	
log2_Ratio_si/c_0h	Fold changes (Log ratio) obtained from DNA microarray, 2D-DIGE, iTRAQ (ESI / MALDI) data at each time point
log2_Ratio_si/c_24h	
log2_Ratio_si/c_48h	
log2_Ratio_si/c_72h	
Absolute_log2_Ratio_si/c_0h	Fold changes (absolute value of Log ratio) obtained from DNA microarray, 2D-DIGE, iTRAQ (ESI / MALDI) data at each time point
Absolute_log2_Ratio_si/c_24h	
Absolute_log2_Ratio_si/c48h	
Absolute_log2_Ratio_si/c72h	
iPEACH_Sum	iPEACH score 1, the sum of fold changes obtained from DNA

	microarray, 2D-DIGE and iTRAQ (ESI / MALDI) data
iPEACH_log2	iPEACH score 2, the sum of fold changes (Log ratio) obtained from DNA microarray, 2D-DIGE and iTRAQ (ESI / MALDI) data
iPEACH_Index*	iPEACH score 3, the sum of fold changes (absolute value of Log ratio) obtained from DNA microarray, 2D-DIGE and iTRAQ (ESI / MALDI) data
Modification	Post Translational Modifications identified by 2D-DIGE, iTRAQ analysis
Cleavage	Protein cleavage sites identified by 2D-DIGE, iTRAQ
Organism	Organism
AA_Seq_Length	Amino acid length
Theoretical_MW	Theoretical MW (kDa) of proteins
Observed_MW	Observed MW (kDa) of proteins identified by 2D-DIGE
Theoretical_pI	Theoretical pI of proteins
Observed_pI	Observed pI of proteins identified in 2D-DIGE
Keyword	Description in SwissProt (keyword)
GO_Biological_Process	Related terms of Gene Ontology Annotation (Biological Process)
GO_Molecular_Function	Related terms of Gene Ontology Annotation (Molecular Function)
GO_Cellular_Component	Related terms of Gene Ontology Annotation (Cellular Components)
SwissProt:[CC]	Description in SwissProt (CC line | CATALYTIC ACTIVITY | INTERACTION | SUBCELLULAR LOCATION | PATHWAY | PTM | TISSUE SPECIFICITY | | SIMILARITY |
SwissProt:[FT]	Description in SwissProt (FT line | SIGNAL | DOMAIN | MOTIF | TRANSMEM | BINDING | CARBOHYD | NP_BIND | MOD_RES | DISULFID | CROSSLNK |)

Table S2

List of proteins identified using nanoLC-MALDI-TOF/TOF and Protein Pilot for the iTRAQ analysis.

iTRAQ ratios were obtained from the ratio of protein expression in the NF1 siRNA treatment to control siRNA treatment groups after 1, 24, 48, and 72 h of NGF treatments

Table S3

List of proteins identified using nano-LC-ESI-Qq-TOF and Protein Pilot for the iTRAQ analysis.

iTRAQ ratios were obtained from the ratio of protein expression in the NF1 siRNA treatment to

control siRNA treatment groups after 1, 24, 48, and 72 h of NGF treatments

Table S4

List of proteins identified by 2D-DIGE.

* the protein spot identified with infusion MALDI-TOF-TOF analysis;

** the protein spot already identified by 2D-DIGE pH 3-11.

Table S5

List of identified dynein IC2 protein isomers with the spot (1, 2, 3, 4, and 5) information. Mascot search was performed with the database focused on the amino acid sequences of RAT_Dynein1IC2 , RAT_Dynein1IC2_Isoform_2B and RAT_Dynein1IC2_Isoform_2C.

Table S6

List of up-/downregulated molecules in NF1 KD cells subjected to the pathway analysis

Table S6-A, the upregulated molecules identified by DNA array

Table S6-B, the upregulated molecules identified by iTRAQ

Table S6-C, the upregulated molecules identified by 2D-DIGE

Table S6-D, the downregulated molecules identified by DNA array

Table S6-E, the downregulated molecules identified by iTRAQ

Table S6-F, the downregulated molecules identified by 2D-DIGE

In 2D-DIGE data, the maximum ratio data for upregulated molecules or the minimum ratio data for downegulated molecules in the all proteins identified from the multiple protein spots with same IDs was adopted to the analysis.

Table S7

List of upregulated molecules in NF1 KD cells subjected to the network analysis.

Table S7-A, the upregulated molecules identified by DNA array

Table S7-B, the upregulated molecules identified by iTRAQ

Table S7-C, the upregulated molecules identified by 2D-DIGE

In 2D-DIGE data, the maximum ratio data in the all proteins with same IDs identified from the multiple protein spots was adopted to the analysis.

Supplemental Figures

Figure S1. Effects of NF1 siRNA on neurite outgrowth of PC12 cells.

A. Immunoblot analysis of cell lysates extracted from PC12 cells transfected with NF1 (249) siRNA, NF1 (611) siRNA, or control siRNA. Cells were harvested after 48 h-NGF treatment, and the lysates were analyzed by immunoblotting with anti-neurofibromin antibodies. Beta-tubulin was used as the internal loading control. A representative image of three independent experiments is shown.

B. Immunoblot analysis of cell lysates extracted from PC12 cells transfected with NF1 (249) siRNA or control siRNA. Cell lysates were prepared at the indicated time points. Beta-tubulin was used as the internal loading control. A representative image of three independent experiments is shown.

C. Immunocytochemistry of NF1-KD PC12 cells. PC12 cells were transfected with control siRNA or NF1 (249) siRNA and stimulated NGF for 72 h. Cells were fixed and incubated with rabbit anti-NF1 antibodies (4 μg/ml), followed by reaction with Alexa 568-conjugated anti-rabbit IgG antibody (red), and observed with a fluorescence microscope. Arrows indicate the inhibition of neurite outgrowth in PC12 cells.

Figure S2. The number of proteins/genes detected by integrated proteomics

The table shows the number of detected proteins/genes obtained in each of the differential (up/downregulated) expression analyses, 2D-DIGE (A), iTRAQ (B), and DNA array (C). The ratios (NF1 siRNA/control) of these data were used for fold-change analysis. For fold-change analysis, if the same protein was identified at several spots found in 2D-DIGE, a maximum/minimum ratio in all detected spots was adopted. The differential analysis of 2D-DIGE was performed using the data for proteins that were up/downregulated at more than one time point.

Figure S3. Identification of dynein IC2 using ProQ-Diamond staining and MS/MS analyses.

A. A pool of all samples used for 2D-DIGE analysis (150 μg) was subjected to phospho-2D-PAGE analysis. Dynein IC2s separated on 2D gels were stained with ProQ-Diamond (green) and SYPRO Ruby (red) and scanned with a Typhoon 9400 imaging system. The merged spots with yellow color (spots 1, 2, and 4) indicate phosphorylated dynein IC2s stained by ProQ-Diamond.

B. Amino acid sequence alignment of three dynein IC2 isoforms identified by nano-LC-ESI-Qq-TOF analysis. Colored boxes indicate peptide sequences that identified each dynein IC2 spot, and asterisks show the phosphorylation sites. Information on the identified peptide and phosphorylated peptides is described in **Supplemental Table S5** and **Supplemental Fig. S3C**

(a)-(c). The red frame shows the area including two alternative splicing sites.

C. (a)-(c) The phosphorylation sites of dynein IC2 identified by nano-LC-ESI-Qq-TOF. Mascot search was performed using the UniProt Rat database including dynein IC2-A, IC2-B, IC2-C.

D. Two siRNA sequence designs specific for dynein IC2-C. The three sequence alignments of a portion of the alternative splicing sites in the rat dynein IC2 isoforms IC2-A (Q62871), IC2-B (Q62871-2), and IC2-C (Q62871-3). The inset indicates the amino acid and corresponding nucleic acid sequences on the alternative splicing site specific for dynein IC2-C. Two specific dynein IC2-C siRNAs were designed using the sequences straddling the splicing site.

E. Effects of dynein IC2-C siRNAs on PC12 cells. PC12 cells were transfected with dynein IC2-C (329), dynein IC2-C (331), or control siRNA and harvested after 24-h transfection. The cell lysates were subjected to analysis with 2D-immunoblotting using anti-dynein IC2 antibody. Arrows indicate the dynein IC2-C spots.

Figure S4. Effects of pan-dynein IC2 siRNA on PC12 neurite outgrowth.

A. Differential interference contrast images of siRNA-treated PC12 cells. Cells were transfected with control siRNA, NF1 (249) siRNA, or both with NF1 (249) and pan-dynein IC2 siRNAs. After 72-h NGF treatment, the morphologies of PC12 cells were observed microscopically.

B. Immunoblot analysis showing that pan-dynein IC2-pan siRNA effectively suppresses all dynein IC2 expression.

C. COX-1 expression is affected by dynein IC2-C siRNA treatment in NF1-KD PC12 cells. Cells were transfected for 24 h with control siRNA, NF1 (249) siRNA, or both NF1 (249) and dynein IC2-C (329 or 331) siRNAs before treatment with NGF. After 48-h NGF treatment, cells were harvested, and lysates were subjected to immunoblot analysis using anti-COX-1 antibody.

Supplemental Figure.1

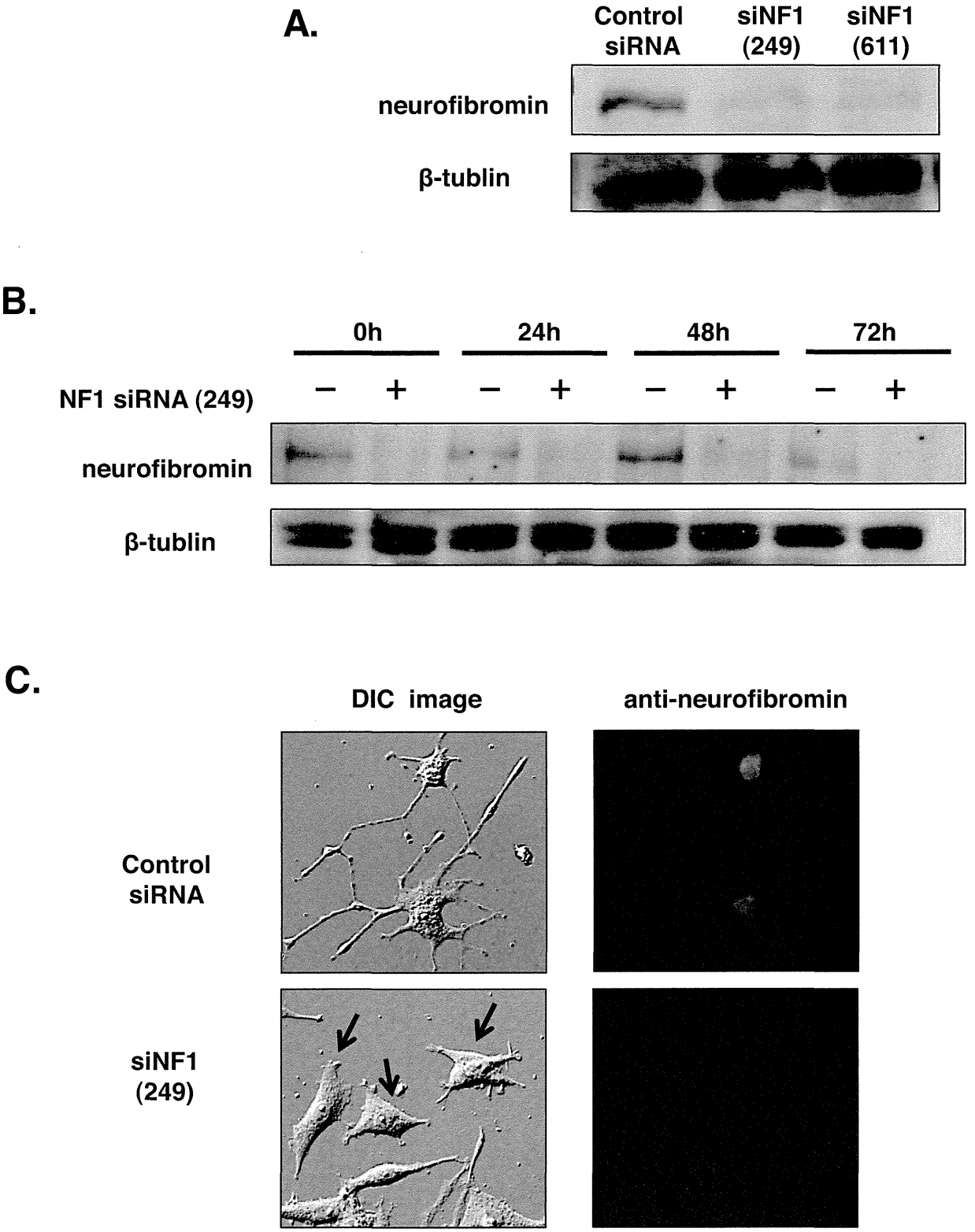

Supplemental Figure.2

A. 2D-DIGE

	pH 3-11	pH 4-7
detected spots	4157	4007
2way ANOVA analysis ($p < 0.05$)	147	187
identified proteins by MS/MS analysis	128	124
up-regulated proteins	32	
down-regulated proteins	20	

B. iTRAQ (MALDI+ESI)

detected 3239 proteins		
time	Down (<0.83)	Up (>1.20)
0h	158	150
24h	126	158
48h	97	135
72h	179	112

C. DNA array

detected 10868 genes		
time	Down (<0.67)	Up (>1.50)
0h	481	603
24h	578	392
48h	375	488
72h	778	401

Supplemental Figure.3

A.

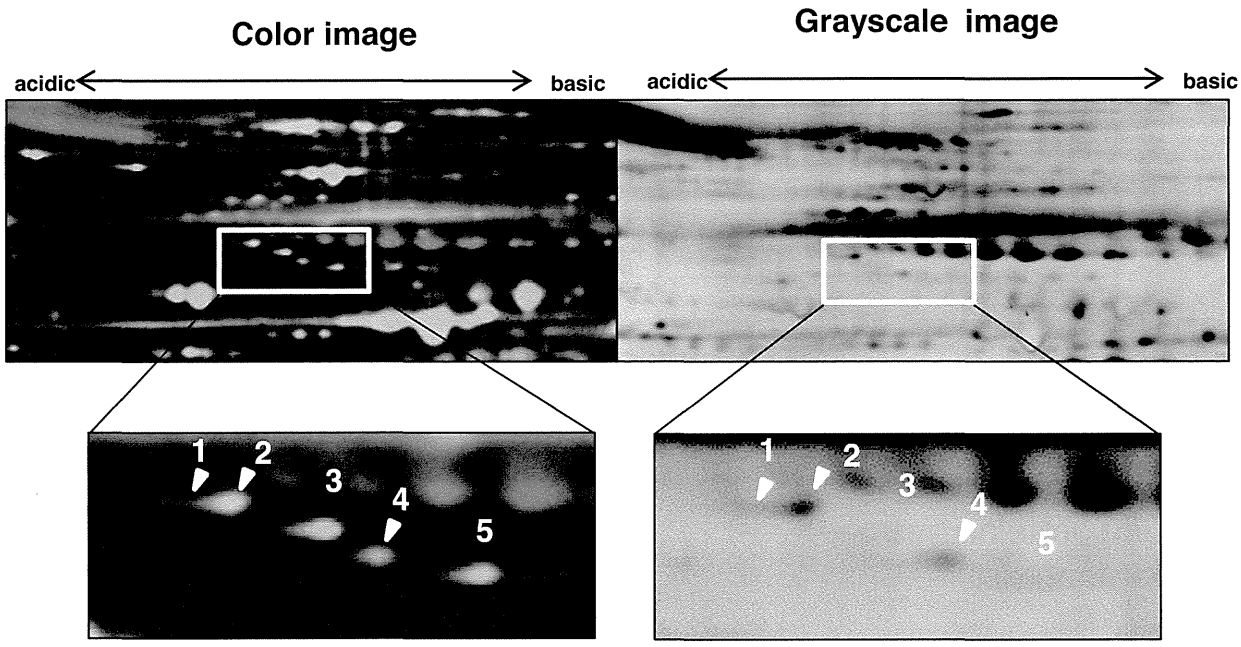

B.

```
sp|Q62871|DC1I2_RAT      1 MSDKSELKAELERKKQRLAQIREEKKRKEEERKKKETDQKKEAAVSVQEESDLEKKRREA 60
sp|Q62871-2|DC1I2_RAT    1 MSDKSELKAELERKKQRLAQIREEKKRKEEERKKKETDQKKEAAVSVQEESDLEKKRREA 60
sp|Q62871-3|DC1I2_RAT    1 MSDKSELKAELERKKQRLAQIREEKKRKEEERKKKETDQKKEAAVSVQEESDLEKKRREA 60

                                                  *  *
sp|Q62871|DC1I2_RAT     61 EALLQSMGLTTDSPIVFSEHWVPPPMSPSSKSVSTPSEAGSQDSGDGAVGSRTLHWDTDP 120
sp|Q62871-2|DC1I2_RAT   61 EALLQSMGLTTDSPI------VPPPMSPSSKSVSTPSEAGSQDSGDGAVGSRTLHWDTDP 114
sp|Q62871-3|DC1I2_RAT   61 EALLQSMGLTTDSPI------VPPPMSPSSKSVSTPSEAGSQDSGDGAVGSR-------- 106

sp|Q62871|DC1I2_RAT    121 SALQLHSDSDLGRGPIKLGMAKITQVDFPPREIVTYTKETQTPVTAQPKEDEEEEDDVAA 180
sp|Q62871-2|DC1I2_RAT  115 SALQLHSDSDLGRGPIKLGMAKITQVDFPPREIVTYTKETQTPVTAQPKEDEEEEDDVAA 174
sp|Q62871-3|DC1I2_RAT  107 ------------RGPIKLGMAKITQVDFPPREIVTYTKETQTPVTAQPKEDEEEEDDVAA 154

sp|Q62871|DC1I2_RAT    181 PKPPVEPEEEKILKKDEENDSKAPPHELTEEEKQQILHSEEFLSFFDHSTRIVERALSEQ 240
sp|Q62871-2|DC1I2_RAT  175 PKPPVEPEEEKILKKDEENDSKAPPHELTEEEKQQILHSEEFLSFFDHSTRIVERALSEQ 234
sp|Q62871-3|DC1I2_RAT  155 PKPPVEPEEEKILKKDEENDSKAPPHELTEEEKQQILHSEEFLSFFDHSTRIVERALSEQ 214

sp|Q62871|DC1I2_RAT    241 INIFFDYSGRDLEDKEGEIQAGAKLSLNRQFFDERWSKHRVVSCLDWSSQYPELLVASYN 300
sp|Q62871-2|DC1I2_RAT  235 INIFFDYSGRDLEDKEGEIQAGAKLSLNRQFFDERWSKHRVVSCLDWSSQYPELLVASYN 294
sp|Q62871-3|DC1I2_RAT  215 INIFFDYSGRDLEDKEGEIQAGAKLSLNRQFFDERWSKHRVVSCLDWSSQYPELLVASYN 274

sp|Q62871|DC1I2_RAT    301 NNEEAPHEPDGVALVWNMKYKKTTPEYVFHCQSAVMSATFAKFHPNLVVGGTYSGQIVLW 360
sp|Q62871-2|DC1I2_RAT  295 NNEEAPHEPDGVALVWNMKYKKTTPEYVFHCQSAVMSATFAKFHPNLVVGGTYSGQIVLW 354
sp|Q62871-3|DC1I2_RAT  275 NNEEAPHEPDGVALVWNMKYKKTTPEYVFHCQSAVMSATFAKFHPNLVVGGTYSGQIVLW 334

sp|Q62871|DC1I2_RAT    361 DNRSNKRTPVQRTPLSAAAHTHPVYCVNVVGTQNAHNLISISTDGKICSWSLDMLSHPQD 420
sp|Q62871-2|DC1I2_RAT  355 DNRSNKRTPVQRTPLSAAAHTHPVYCVNVVGTQNAHNLISISTDGKICSWSLDMLSHPQD 414
sp|Q62871-3|DC1I2_RAT  335 DNRSNKRTPVQRTPLSAAAHTHPVYCVNVVGTQNAHNLISISTDGKICSWSLDMLSHPQD 394

sp|Q62871|DC1I2_RAT    421 SMELVHKQSKAVAVTSMSFPVGDVNNFVVGSEEGSVYTACRHGSKAGISEMFEGHQGPIT 480
sp|Q62871-2|DC1I2_RAT  415 SMELVHKQSKAVAVTSMSFPVGDVNNFVVGSEEGSVYTACRHGSKAGISEMFEGHQGPIT 474
sp|Q62871-3|DC1I2_RAT  395 SMELVHKQSKAVAVTSMSFPVGDVNNFVVGSEEGSVYTACRHGSKAGISEMFEGHQGPIT 454

sp|Q62871|DC1I2_RAT    481 GIHCHAAVGAVDFSHLFVTSSFDWTVKLWSTKNNKPLYSFEDNSDYVYDVIGSPTHPALF 540
sp|Q62871-2|DC1I2_RAT  475 GIHCHAAVGAVDFSHLFVTSSFDWTVKLWSTKNNKPLYSFEDNSDYVYDVIGSPTHPALF 534
sp|Q62871-3|DC1I2_RAT  455 GIHCHAAVGAVDFSHLFVTSSFDWTVKLWSTKNNKPLYSFEDNSDYVYDVIGSPTHPALF 514

sp|Q62871|DC1I2_RAT    541 ACVDGMGRLDLWNLNNDTEVPTASISVEGNPALNRVRWTHSGREIAVGDSEGQIVIYDVG 600
sp|Q62871-2|DC1I2_RAT  535 ACVDGMGRLDLWNLNNDTEVPTASISVEGNPALNRVRWTHSGREIAVGDSEGQIVIYDVG 594
sp|Q62871-3|DC1I2_RAT  515 ACVDGMGRLDLWNLNNDTEVPTASISVEGNPALNRVRWTHSGREIAVGDSEGQIVIYDVG 574

sp|Q62871|DC1I2_RAT    601 EQIAVPRNDEWARFGRTLAEINASRADAEEEAATRIPA                       638
sp|Q62871-2|DC1I2_RAT  595 EQIAVPRNDEWARFGRTLAEINASRADAEEEAATRIPA                       632
sp|Q62871-3|DC1I2_RAT  575 EQIAVPRNDEWARFGRTLAEINASRADAEEEAATRIPA                       612
```

*** phosphorylation site**

color	spot
pink	1 , 2
blue	3
orange	4
green	5
purple	2 and 3
Yellow green	4 and 5

Supplemental Figure 3C-(a)

Master Spot No.1917

position S87

Match to Query 220: 2894.435061 from(965.818963,3+)
Monoisotopic mass of neutral peptide Mr(calc): 2894.33
Variable modifications:
M9 : Oxidation (M)
M22 : Oxidation (M)
S23 : Phospho (ST), with neutral losses 97.98(shown in table), 0.00
Ions Score: 28 Expect: 0.00043

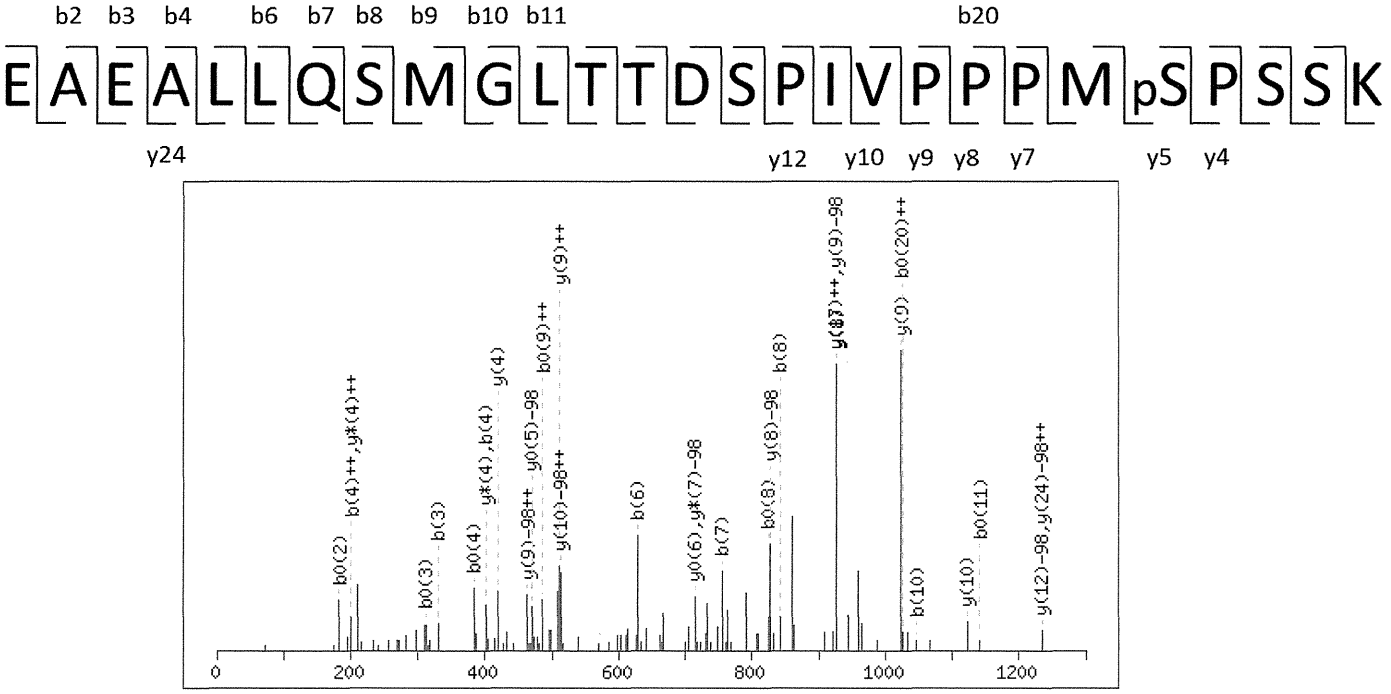

#	b	b^{++}	b*	b^{*++}	b^{0}	b^{0++}	Seq.	y	y^{++}	y*	y^{*++}	y^{0}	y^{0++}	#
1	130.05	65.53			112.04	56.52	E							27
2	201.09	101.05			183.08	92.04	A	2668.32	1334.66	2651.29	1326.15	2650.31	1325.66	26
3	330.13	165.57			312.12	156.56	E	2597.28	1299.15	2580.26	1290.63	2579.27	1290.14	25
4	401.17	201.09			383.16	192.08	A	2468.24	1234.62	2451.21	1226.11	2450.23	1225.62	24
5	514.25	257.63			496.24	248.62	L	2397.2	1199.11	2380.18	1190.59	2379.19	1190.1	23
6	627.33	314.17			609.32	305.17	L	2284.12	1142.56	2267.09	1134.05	2266.11	1133.56	22
7	755.39	378.2	738.37	369.69	737.38	369.2	Q	2171.04	1086.02	2154.01	1077.51	2153.03	1077.02	21
8	842.43	421.72	825.4	413.2	824.41	412.71	S	2042.98	1021.99	2025.95	1013.48	2024.97	1012.99	20
9	989.46	495.23	972.43	486.72	971.45	486.23	M	1955.95	978.48	1938.92	969.96	1937.93	969.47	19
10	1046.48	523.74	1029.46	515.23	1028.47	514.74	G	1808.91	904.96	1791.88	896.45	1790.9	895.95	18
11	1159.57	580.29	1142.54	571.77	1141.56	571.28	L	1751.89	876.45	1734.86	867.93	1733.88	867.44	17
12	1260.61	630.81	1243.59	622.3	1242.6	621.81	T	1638.8	819.91	1621.78	811.39	1620.79	810.9	16
13	1361.66	681.33	1344.64	672.82	1343.65	672.33	T	1537.76	769.38	1520.73	760.87	1519.75	760.38	15
14	1476.69	738.85	1459.66	730.33	1458.68	729.84	D	1436.71	718.86	1419.68	710.34	1418.7	709.85	14
15	1563.72	782.36	1546.69	773.85	1545.71	773.36	S	1321.68	661.34	1304.66	652.83	1303.67	652.34	13
16	1660.77	830.89	1643.75	822.38	1642.76	821.89	P	1234.65	617.83	1217.62	609.32	1216.64	608.82	12
17	1773.86	887.43	1756.83	878.92	1755.85	878.43	I	1137.6	569.3	1120.57	560.79	1119.59	560.3	11
18	1872.93	936.97	1855.9	928.45	1854.92	927.96	V	1024.51	512.76	1007.49	504.25	1006.5	503.75	10
19	1969.98	985.49	1952.95	976.98	1951.97	976.49	P	925.44	463.23	908.42	454.71	907.43	454.22	9
20	2067.03	1034.02	2050	1025.51	2049.02	1025.01	P	828.39	414.7	811.37	406.19	810.38	405.69	8
21	2164.08	1082.55	2147.06	1074.03	2146.07	1073.54	P	731.34	366.17	714.31	357.66	713.33	357.17	7
22	2311.12	1156.06	2294.09	1147.55	2293.11	1147.06	M	634.29	317.65	617.26	309.13	616.28	308.64	6
23	2380.14	1190.57	2363.11	1182.06	2362.13	1181.57	S	487.25	244.13	470.22	235.62	469.24	235.12	5
24	2477.19	1239.1	2460.17	1230.59	2459.18	1230.1	P	418.23	209.62	401.2	201.11	400.22	200.61	4
25	2564.23	1282.62	2547.2	1274.1	2546.22	1273.61	S	321.18	161.09	304.15	152.58	303.17	152.09	3
26	2651.26	1326.13	2634.23	1317.62	2633.25	1317.13	S	234.14	117.58	217.12	109.06	216.13	108.57	2
27							K	147.11	74.06	130.09	65.55			1

Supplemental Figure3C-(b)

Master Spot No.1988

position S87

Match to Query 158: 2894.351943 from(965.791257,3+)
Monoisotopic mass of neutral peptide Mr(calc): 2894.33
Variable modifications:
M9 : Oxidation (M)
M22 : Oxidation (M)
S23 : Phospho (ST), with neutral losses 97.98(shown in table), 0.00
Ions Score: 36 Expect: 6.8e-005

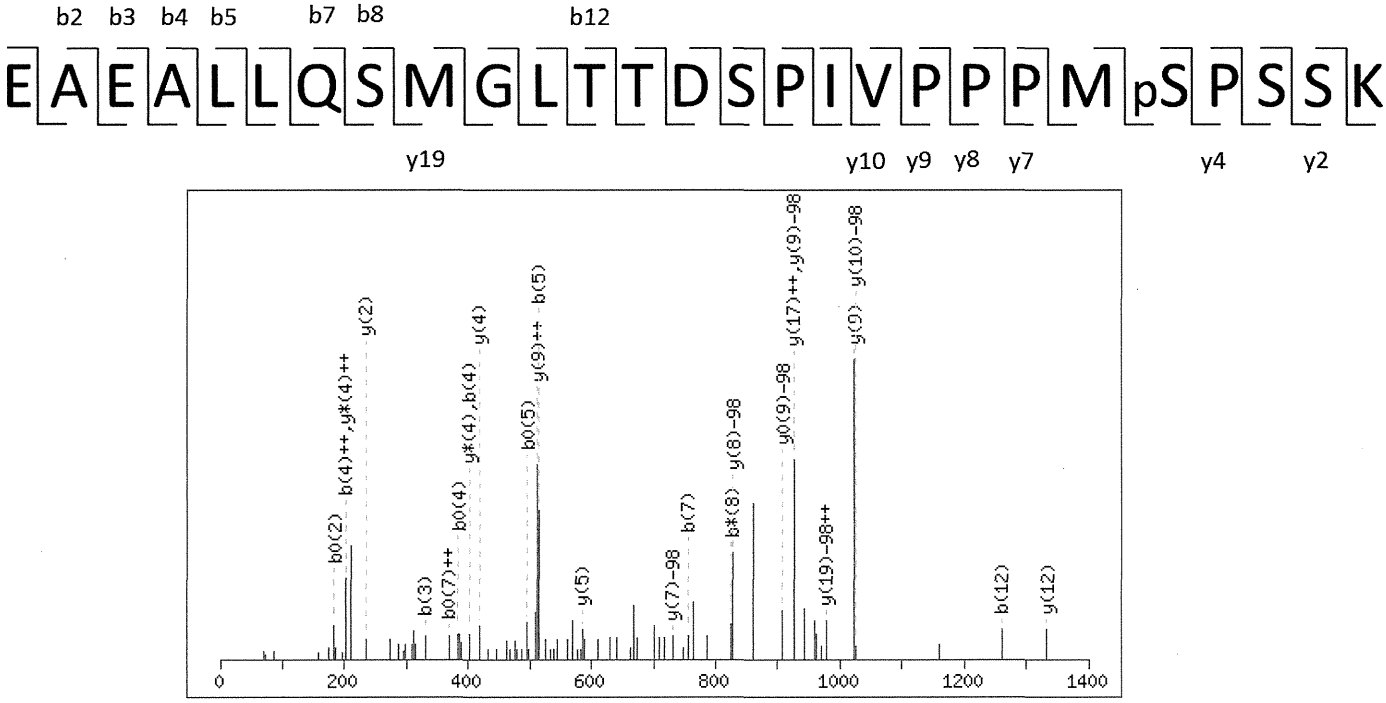

#	b	b^{++}	b*	b^{*++}	b^{0}	b^{0++}	Seq.	y	y^{++}	y*	y^{*++}	y^{0}	y^{0++}	#
1	130.05	65.53			112.04	56.52	E							27
2	201.09	101.05			183.08	92.04	A	2668.32	1334.66	2651.29	1326.15	2650.31	1325.66	26
3	330.13	165.57			312.12	156.56	E	2597.28	1299.15	2580.26	1290.63	2579.27	1290.14	25
4	401.17	201.09			383.16	192.08	A	2468.24	1234.62	2451.21	1226.11	2450.23	1225.62	24
5	514.25	257.63			496.24	248.62	L	2397.2	1199.11	2380.18	1190.59	2379.19	1190.1	23
6	627.33	314.17			609.32	305.17	L	2284.12	1142.56	2267.09	1134.05	2266.11	1133.56	22
7	755.39	378.2	738.37	369.69	737.38	369.2	Q	2171.04	1086.02	2154.01	1077.51	2153.03	1077.02	21
8	842.43	421.72	825.4	413.2	824.41	412.71	S	2042.98	1021.99	2025.95	1013.48	2024.97	1012.99	20
9	989.46	495.23	972.43	486.72	971.45	486.23	M	1955.95	978.48	1938.92	969.96	1937.93	969.47	19
10	1046.48	523.74	1029.46	515.23	1028.47	514.74	G	1808.91	904.96	1791.88	896.45	1790.9	895.95	18
11	1159.57	580.29	1142.54	571.77	1141.56	571.28	L	1751.89	876.45	1734.86	867.93	1733.88	867.44	17
12	1260.61	630.81	1243.59	622.3	1242.6	621.81	T	1638.8	819.91	1621.78	811.39	1620.79	810.9	16
13	1361.66	681.33	1344.64	672.82	1343.65	672.33	T	1537.76	769.38	1520.73	760.87	1519.75	760.38	15
14	1476.69	738.85	1459.66	730.33	1458.68	729.84	D	1436.71	718.86	1419.68	710.34	1418.7	709.85	14
15	1563.72	782.36	1546.69	773.85	1545.71	773.36	S	1321.68	661.34	1304.66	652.83	1303.67	652.34	13
16	1660.77	830.89	1643.75	822.38	1642.76	821.89	P	1234.65	617.83	1217.62	609.32	1216.64	608.82	12
17	1773.86	887.43	1756.83	878.92	1755.85	878.43	I	1137.6	569.3	1120.57	560.79	1119.59	560.3	11
18	1872.93	936.97	1855.9	928.45	1854.92	927.96	V	1024.51	512.76	1007.49	504.25	1006.5	503.75	10
19	1969.98	985.49	1952.95	976.98	1951.97	976.49	P	925.44	463.23	908.42	454.71	907.43	454.22	9
20	2067.03	1034.02	2050	1025.51	2049.02	1025.01	P	828.39	414.7	811.37	406.19	810.38	405.69	8
21	2164.08	1082.55	2147.06	1074.03	2146.07	1073.54	P	731.34	366.17	714.31	357.66	713.33	357.17	7
22	2311.12	1156.06	2294.09	1147.55	2293.11	1147.06	M	634.29	317.65	617.26	309.13	616.28	308.64	6
23	2380.14	1190.57	2363.11	1182.06	2362.13	1181.57	S	487.25	244.13	470.22	235.62	469.24	235.12	5
24	2477.19	1239.1	2460.17	1230.59	2459.18	1230.1	P	418.23	209.62	401.2	201.11	400.22	200.61	4
25	2564.23	1282.62	2547.2	1274.1	2546.22	1273.61	S	321.18	161.09	304.15	152.58	303.17	152.09	3
26	2651.26	1326.13	2634.23	1317.62	2633.25	1317.13	S	234.14	117.58	217.12	109.06	216.13	108.57	2
27							K	147.11	74.06	130.09	65.55			1

Supplemental Figure3C-(c)

Master Spot No.2069

position S87

Match to Query 236: 2894.330043 from(965.783957,3+)
Monoisotopic mass of neutral peptide Mr(calc): 2894.33
Variable modifications:
M9 : Oxidation (M)
M22 : Oxidation (M)
S23 : Phospho (ST), with neutral losses 97.98(shown in table), 0.00
Ions Score: 49 Expect: 3.4e-006

b2 b3 b4 b5 b6 b7 b8 b10 b12 b15

E A E A L L Q S M G L T T D S P I V P P P M pS P S S K

y12 y9 y8 y7 y6 y5 y4 y2 y1

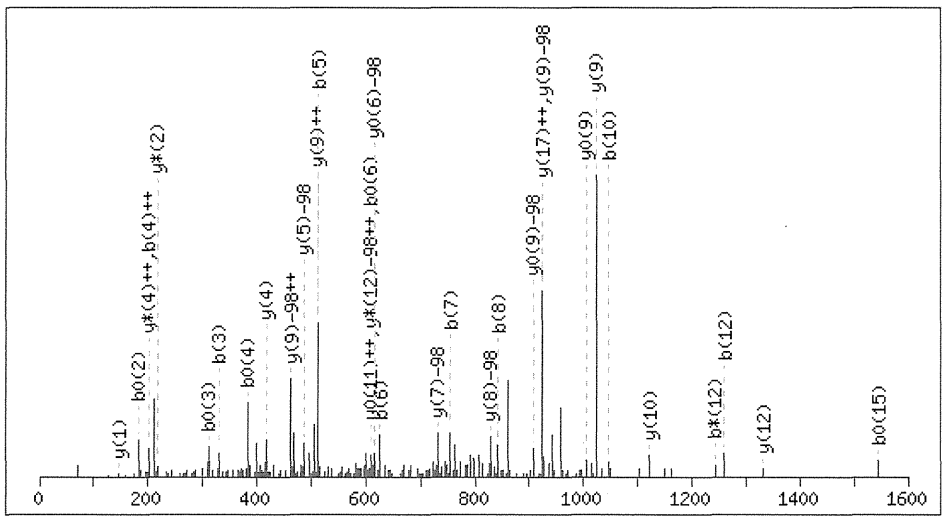

#	b	b^{++}	b*	b^{*++}	b^{0}	b^{0++}	Seq.	y	y^{++}	y*	y^{*++}	y^{0}	y^{0++}	#
1	130.05	65.53			112.04	56.52	E							27
2	201.09	101.05			183.08	92.04	A	2668.32	1334.66	2651.29	1326.15	2650.31	1325.66	26
3	330.13	165.57			312.12	156.56	E	2597.28	1299.15	2580.26	1290.63	2579.27	1290.14	25
4	401.17	201.09			383.16	192.08	A	2468.24	1234.62	2451.21	1226.11	2450.23	1225.62	24
5	514.25	257.63			496.24	248.62	L	2397.2	1199.11	2380.18	1190.59	2379.19	1190.1	23
6	627.33	314.17			609.32	305.17	L	2284.12	1142.56	2267.09	1134.05	2266.11	1133.56	22
7	755.39	378.2	738.37	369.69	737.38	369.2	Q	2171.04	1086.02	2154.01	1077.51	2153.03	1077.02	21
8	842.43	421.72	825.4	413.2	824.41	412.71	S	2042.98	1021.99	2025.95	1013.48	2024.97	1012.99	20
9	989.46	495.23	972.43	486.72	971.45	486.23	M	1955.95	978.48	1938.92	969.96	1937.93	969.47	19
10	1046.48	523.74	1029.46	515.23	1028.47	514.74	G	1808.91	904.96	1791.88	896.45	1790.9	895.95	18
11	1159.57	580.29	1142.54	571.77	1141.56	571.28	L	1751.89	876.45	1734.86	867.93	1733.88	867.44	17
12	1260.61	630.81	1243.59	622.3	1242.6	621.81	T	1638.8	819.91	1621.78	811.39	1620.79	810.9	16
13	1361.66	681.33	1344.64	672.82	1343.65	672.33	T	1537.76	769.38	1520.73	760.87	1519.75	760.38	15
14	1476.69	738.85	1459.66	730.33	1458.68	729.84	D	1436.71	718.86	1419.68	710.34	1418.7	709.85	14
15	1563.72	782.36	1546.69	773.85	1545.71	773.36	S	1321.68	661.34	1304.66	652.83	1303.67	652.34	13
16	1660.77	830.89	1643.75	822.38	1642.76	821.89	P	1234.65	617.83	1217.62	609.32	1216.64	608.82	12
17	1773.86	887.43	1756.83	878.92	1755.85	878.43	I	1137.6	569.3	1120.57	560.79	1119.59	560.3	11
18	1872.93	936.97	1855.9	928.45	1854.92	927.96	V	1024.51	512.76	1007.49	504.25	1006.5	503.75	10
19	1969.98	985.49	1952.95	976.98	1951.97	976.49	P	925.44	463.23	908.42	454.71	907.43	454.22	9
20	2067.03	1034.02	2050	1025.51	2049.02	1025.01	P	828.39	414.7	811.37	406.19	810.38	405.69	8
21	2164.08	1082.55	2147.06	1074.03	2146.07	1073.54	P	731.34	366.17	714.31	357.66	713.33	357.17	7
22	2311.12	1156.06	2294.09	1147.55	2293.11	1147.06	M	634.29	317.65	617.26	309.13	616.28	308.64	6
23	2380.14	1190.57	2363.11	1182.06	2362.13	1181.57	S	487.25	244.13	470.22	235.62	469.24	235.12	5
24	2477.19	1239.1	2460.17	1230.59	2459.18	1230.1	P	418.23	209.62	401.2	201.11	400.22	200.61	4
25	2564.23	1282.62	2547.2	1274.1	2546.22	1273.61	S	321.18	161.09	304.15	152.58	303.17	152.09	3
26	2651.26	1326.13	2634.23	1317.62	2633.25	1317.13	S	234.14	117.58	217.12	109.06	216.13	108.57	2
27							K	147.11	74.06	130.09	65.55			1

Supplemental Figure.3

D.

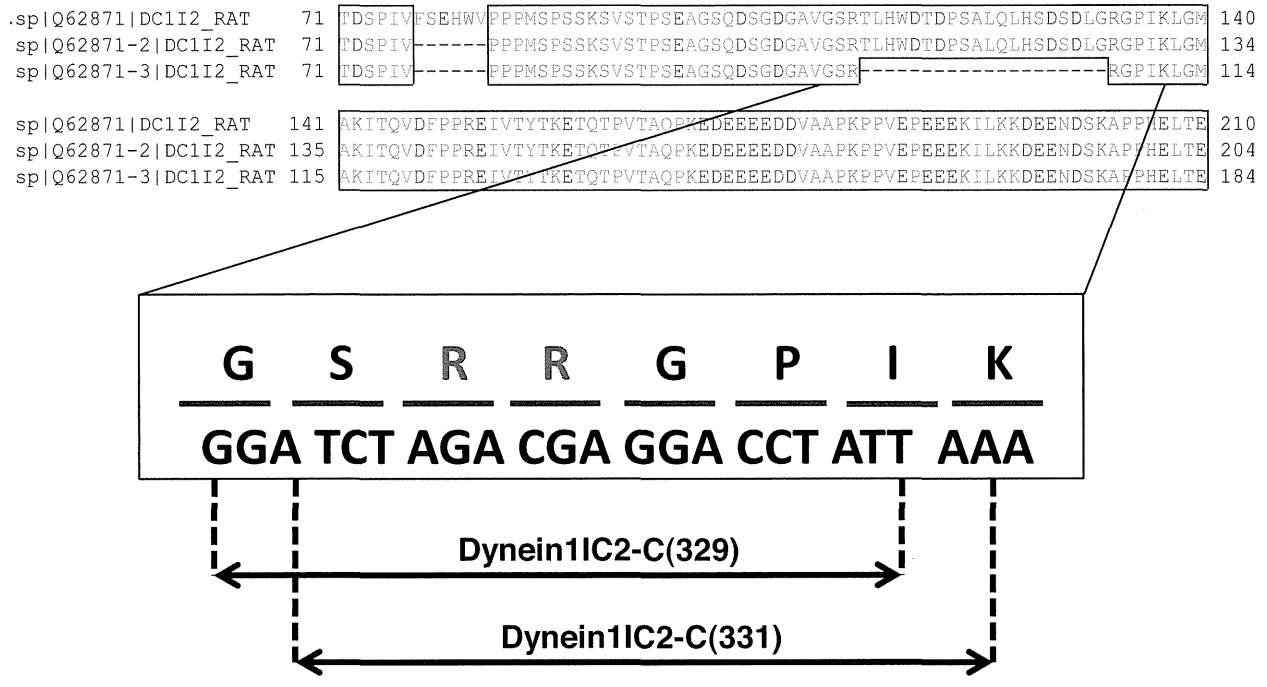

E.

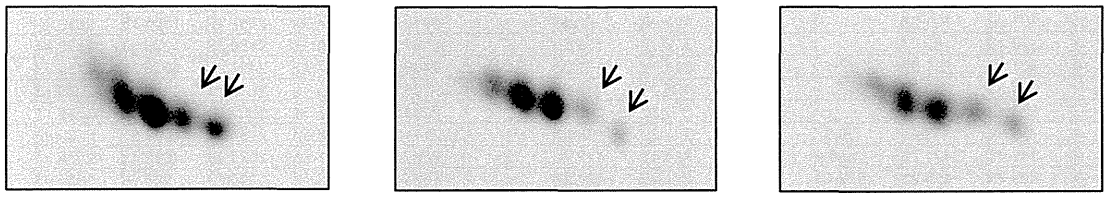

Supplemental Figure.4

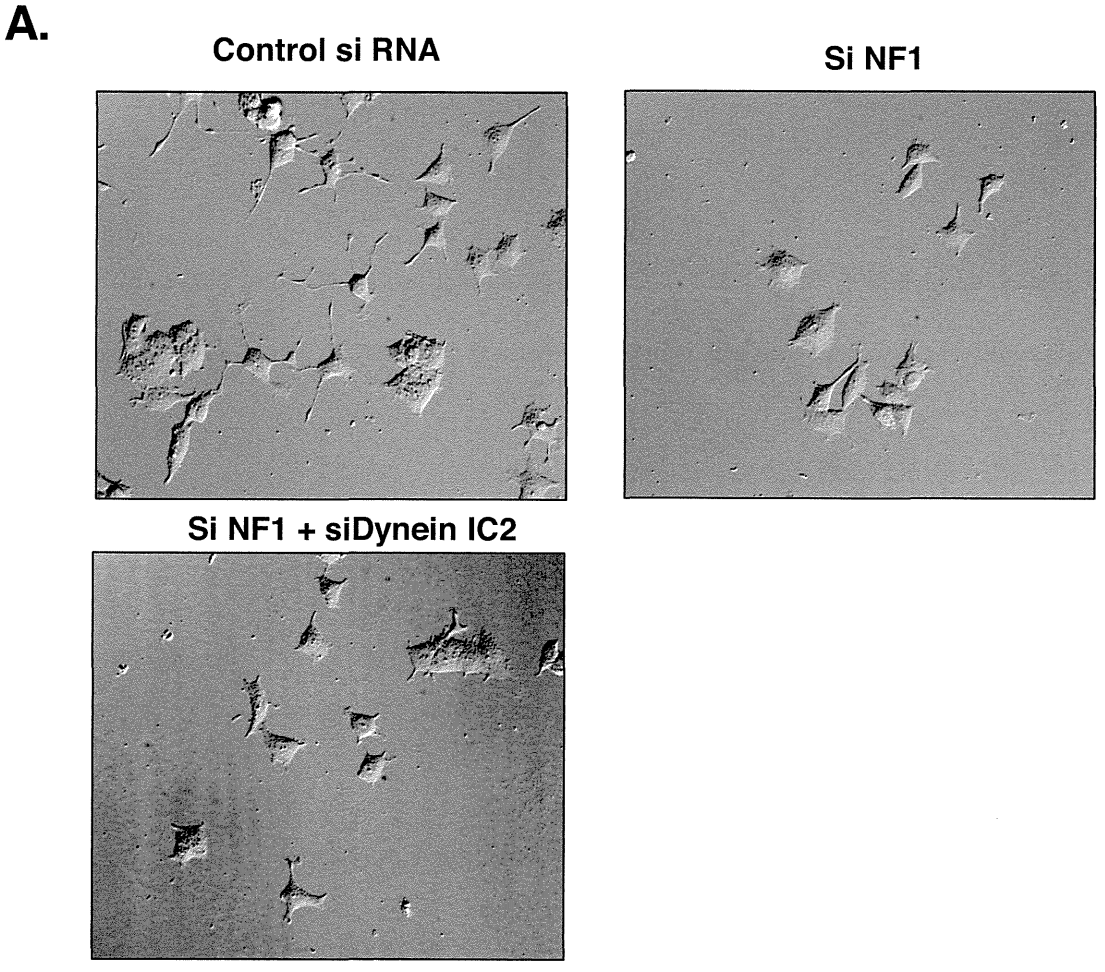

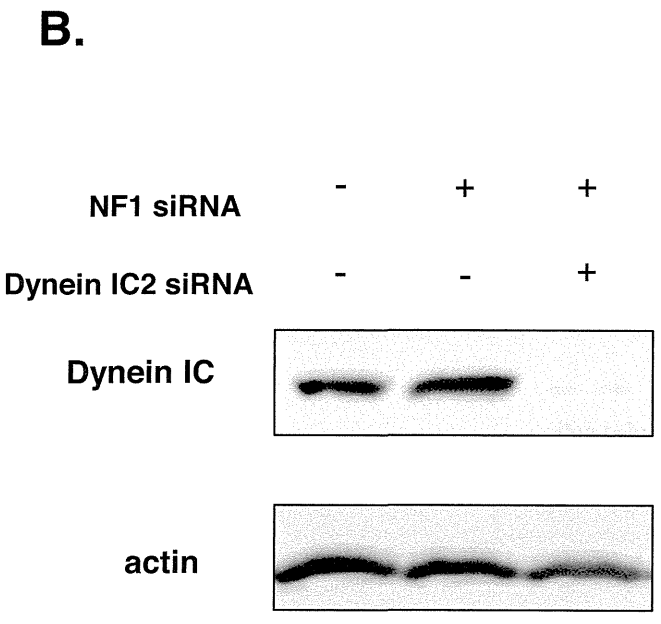

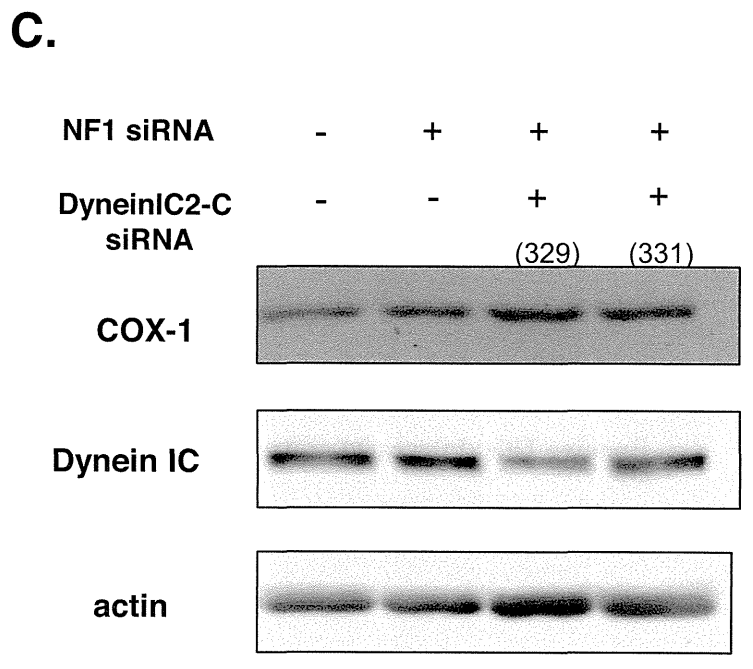

MCP Papers in Press. Published on January 28, 2013 as Manuscript M112.024802

Integrated proteomics identified novel activation of dynein IC2-GR-COX-1 signaling in NF1 disease model cells

Mio Hirayama[1]*, Daiki Kobayashi[1]*, Souhei Mizuguchi[1], Takashi Morikawa[1], Megumi Nagayama[1], Uichi Midorikawa[1], Masayo M. Wilson[1], Akiko N. Nambu[1], Akiyasu C. Yoshizawa[2], Shin Kawano[3], and Norie Araki[1**]

[1]Department of Tumor Genetics and Biology, Graduate school of Medical Sciences, Kumamoto University, 1-1-1, Honjo, Chuo-ku, Kumamoto 860-8556, Japan.

[2]Bioinformatics Center, Institute for Chemical Research, Kyoto University, Gokasho, Uji, Kyoto 611-0011, Japan

[3]Database Center for Life Science, Research Organization of Information and Systems, 2-11-16, Yayoi, Bunkyo-ku, Tokyo 113-0032, Japan

*These authors contributed equally to this work.

**To whom correspondence should be addressed: Norie Araki, Ph. D.

Department of Tumor Genetics and Biology, Graduate school of Medical Sciences,

Kumamoto University, 1-1-1, Honjo, Kumamoto 860-8556, Japan

Tel; +81-96-373-5119, Fax; +81-96-373-5210

E-mail; nori@gpo.kumamoto-u.ac.jp

Running Title: Integrated proteomics of NF1 disease model cells

Abbreviations

NF1-KD, NF1 knockdown; 2D-DIGE, two-dimensional fluorescence difference gel electrophoresis; iTRAQ, isobaric tagging for relative and absolute quantitation; iPEACH, Integrated Protein Expression Analysis Chart; NGF, nerve growth factor; GO, gene ontology; MANGO, Molecular Annotation by Gene Ontology; Qq-TOF, quadrupole/quadrupole/time-of-flight mass spectrometers; dynein IC, dynein intermediate chain; GR, glucocorticoid receptor; COX-1, cyclooxygenase-1; siRNA, short interfering RNA; MPNST, malignant peripheral nerve sheath tumor; PGE2, prostaglandin E2

Foot note

Authors' present addresses;

S Mizuguchi, Dept. Neurosurgery, Faculty of Medicine, University of Miyazaki, 5200 Kihara Kiyotake Miyazaki , 889-1692, Japan

T Morikawa, Mitsubishi Chemical Medience Corporation, 14, Sunayama, Kamisu, Ibaraki 314-0255, Japan.

U. Midorikawa, Healthcare Systems Laboratories, Sharp Corp. 1-9-2, Nakase, Mihama-ku, Chiba, 261-8520, JapanA. C. Yoshizawa, Koichi Tanaka Laboratory of Advanced Science and Technology, Shimadzu Corporation, Nishinokyo-Kuwabara-cho, Nakagyo-ku, Kyoto 604-8511, Japan

Summary

Neurofibromatosis type 1 (NF1) tumor suppressor gene product, neurofibromin, functions in part as a Ras-GAP, and though its loss is implicated in the neuronal abnormality of NF1 patients, its precise cellular function remains unclear. To study the molecular mechanism of NF1 pathogenesis, we prepared NF1 gene knockdown (KD) PC12 cells, as a NF1 disease model, and analyzed their molecular (gene and protein) expression profiles with a unique integrated proteomics approach, comprising iTRAQ, 2D-DIGE, and DNA microarrays, using an integrated protein/gene expression analysis chart (iPEACH). In NF1-KD PC12 cells showing abnormal neuronal differentiation after NGF treatment, of 3198 molecules quantitatively identified and listed in iPEACH, 97 molecules continuously up- or down-regulated over time were extracted. Pathway/network analysis further revealed overrepresentation of calcium signaling and transcriptional regulation by glucocorticoid receptor (GR) in the upregulated protein set, while nerve system development was overrepresented in the downregulated protein set. The novel upregulated network we discovered, "dynein IC2-GR-COX-1 signaling," was then examined in NF1-KD cells. Validation studies confirmed that NF1 knockdown induces altered splicing and phosphorylation patterns of dynein IC2 isomers, upregulation and accumulation of nuclear GR, and increased COX-1 expression in NGF-treated cells. Moreover, the neurite retraction phenotype observed in NF1-KD cells was significantly recovered by knockdown of the dynein IC2-C isoform and COX-1. In addition, dynein IC2 siRNA significantly inhibited nuclear translocation/accumulation of GR and upregulation of COX-1 expression. These results suggest that dynein IC2 upregulates GR nuclear translocation/accumulation, and subsequently causes increased COX-1 expression, in this NF1 disease model. Our integrated proteomics strategy, which combines multiple approaches, demonstrates that NF1-related neural abnormalities are, in part, caused by upregulation of dynein IC2-GR-COX-1

signaling, which may be a novel therapeutic target for NF1.